Biogeosciences Discuss., 8, 8645–8691, 2011
www.biogeosciences-discuss.net/8/8645/2011/
doi:10.5194/bgd-8-8645-2011

Biogeosciences
Discussions

Intercontinental trans-boundary contributions to ozone-induced crop yield losses in the Northern Hemisphere

M. J. Hollaway[1], **S. R. Arnold**[1], **A. J. Challinor**[1], **and L. D. Emberson**[2]

[1]Institute for Climate and Atmospheric Science, School of Earth and Environment,
University of Leeds, Leeds, UK
[2]Stockholm Environment Institute, University of York, York, UK

Received: 26 July 2011 – Accepted: 18 August 2011 – Published: 26 August 2011

Correspondence to: S. R. Arnold (s.arnold@leeds.ac.uk)

Published by Copernicus Publications on behalf of the European Geosciences Union.

Abstract

Enhanced surface ozone concentrations are known to be harmful to vegetation, reducing crop growth and yields. Tropospheric ozone concentrations have increased steadily since pre-industrial times, driven by in-situ production from anthropogenic emissions of nitrogen oxides (NO_x), CO and volatile organic compounds. Transport of ozone and its precursors between continents has been shown to contribute to surface ozone air quality exceedences in many regions of the Northern Hemisphere. Using a global atmospheric chemistry model, we have quantified for the first time, intercontinental contributions to crop ozone exposure and yield reduction in the Northern Hemisphere. We apply three metrics (AOT40/M7/M12) to assess the impacts of NO_x emissions from each of the Northern Hemispheres three major industrialised regions (North (N) America, South East (SE) Asia and Europe) on global and regional exposure of 6 major agricultural crop types to harmful ozone concentrations, and the resultant yield losses during the 2000 growing season. Using these metrics, model calculations show that for wheat, rice, cotton and potato, 100 % reductions in SE Asian anthropogenic NO_x emissions tend to produce the greatest global reduction in crop yield losses (48.8 to 94.7 %) with the same cuts to N American emissions resulting in the greatest global impact on crop yield reductions for maize and soybean (57.5 to 81.7 %). N American NO_x emissions produce the largest transboundary impact, resulting in European yield loss reductions of between 12.4 % and 55.6 %, when a 100 % cut is applied to NO_x emissions from the N American region. European NO_x emissions tend to produce a smaller transboundary impact, due to inefficiency of transport from the European domain. The threshold nature of the AOT40 ozone-exposure metric, results in a strong dependence of the diagnosed impact from trans-boundary emissions on local ozone concentration. In addition, we find that in parts of the United States, biomass burning emissions may make important contributions to ozone-induced crop yield reductions. Our results demonstrate that local air quality and emission control strategies have the potential to partly alleviate ozone-induced crop yield loss in continents downstream, in addition to effectively mitigating local ozone-induced yield losses.

1 Introduction

In recent decades tropospheric ozone has emerged as a global air pollution problem and has been observed to have harmful impacts on vegetation (Fuhrer and Achermann, 1994; Jager et al., 1996; USEPA, 1996) with field experiments showing ozone damage to result in yield reduction and deterioration in crop quality (Fuhrer, 2009). Ozone is produced in-situ in the troposphere through a sequence of sunlight-driven photochemical reactions involving nitrogen oxides ($NO_x = NO + NO_2$) and volatile organic compounds or CO (Crutzen et al., 1999). Since the pre-industrial period, anthropogenic emissions of NO_x and methane have led to increased ambient ozone over many regions (Prather et al., 2001). Ozone-induced crop yield reductions have been suggested to lead to economic loss and to threaten food security, which has become an issue of increasing concern where the expanding economy has resulted in increased emissions of ozone precursors (oxides of nitrogen (NO_x) in particular) from the worlds major industrialized regions (Adams et al., 1982; Aunan et al., 2000; Holland et al., 2002; Li et al., 1999; Wang and Mauzerall, 2004).

Partly in response to this damage, air quality standards (AQS) specifically targeting vegetation have been adopted in Europe (RoyalSociety, 2008), in an aim to reduce surface ozone concentrations to protect vegetation. AQS also exist for human health to which enhanced ozone concentrations are detrimental, however, these tend to focus on different ozone exposure characteristics (short-term peak ozone concentrations rather than longer-term chronic ozone episodes) due to the nature of the impact processes. As such, it is questionable whether human health AQSs will protect ecosystems. The AOT40 (accumulated exposure over a threshold of 40 ppbv) metric has been adopted in Europe (EEA, 1999), to assess ozone exposure risk of vegetation, and has been used in East Asia as well as globally to assess ozone risk (Van Dingenen et al., 2009; Wang and Mauzerall, 2004). The United Nations Economic Commission for Europe (UNECE), and the World Meteorological Organization (WMO) set a critical threshold value of AOT40 at 3 ppm h daylight hour accumulated ozone exposure, which should not be exceeded during the plant growing season (WHO, 2000). In the United States, as of 2007, the USEPA has set equal primary and secondary standards for the protection of human health and human welfare (including damage to crops) respectively, with a peak 8 h mean ozone concentration not to exceed 75 ppbv more than three times a year (USEPA, 2010b). The USEPA is currently in the process of revising these AQS (USEPA, 2010a).

An alternative set of standards developed to assess the impact of ozone exposure on vegetation are M7 and M12 (collectively referred to as Mx), as described in (Tong et al., 2009a). These indices are calculated over 3 consecutive months of a plant growing season as the means of representative daytime 7 h (M7) and 12 h (M12) surface ozone concentrations. These Mx indices differ from AOT40 in that they apply equal weighting to all ozone concentrations to which the plant is exposed, whereas AOT40 only accounts for ozone concentrations above the 40 ppbv threshold. Using Mx also allows estimation of changes in yield losses resulting from ozone concentrations of less than 40 ppbv, although the Mx Weibull relationship used to relate exposure to damage is such that lower ozone concentrations are expected to cause less damage so that a similar, though less severe threshold, still exists. These nuances are important to understand especially since it has been demonstrated that damage to crops can still occur below 40 ppbv ozone exposure (Ashmore, 2005; Sitch et al., 2007) which would otherwise not be accounted for using the AOT40 index.

The Mx indices have been criticized for their inability to characterize different types of exposure regimes, partly as they have the potential to put more emphasis on the more numerous but less biologically significant lower ozone concentrations (Heck and Colwing, 1997). AOT40 differs to Mx in that it emphasizes both the peak ozone concentrations above a threshold (in this case 40 ppbv) as well as the duration of these enhanced ozone levels. As such, the inferred damage will be rather dependent on the diurnal and seasonal ozone concentration profiles and the frequency with which hourly ozone concentrations exceed the threshold set. M7 and M12 have however been used in a number of modelling studies to assess the impact of ozone on crop damage. Tong et al. (2009a) used a number of exposure and concentration based indices (including M7, M12 and AOT40) to assess vegetation exposure to ozone over the United States using an air quality forecast model. M7 and M12 were also used in the US EPAs National Crop Loss Assessment Network (NCLAN) (Heck et al., 1984). Van Dingenen et al. (2009) concluded that AOT40s low robustness (high sensitivity to small changes in ozone concentration close to the 40 ppbv threshold and uncertainties in input values) made it less suitable as an indicator for crop losses in modelling-based studies. They also concluded that M7 performs satisfactorily from a modelling point of view, but is considered a less suitable indicator for crop exposure.

Overall, emissions reductions in response to monitoring of exceedences of standards set in health and vegetation exposure guidelines, have in part resulted in the decrease in the frequency of peak ozone levels since the 1990s (Lin et al., 2001; Soldberg and Lindskog, 2005). However as many economies are still growing rapidly (in particular those in southern and eastern Asia), the emission of ozone precursor trace gases in the Northern Hemisphere (NH) is expected to continue to rise (Zhang et al., 2009). Many observational and modelling studies have quantified contributions to regional surface ozone concentrations from import of ozone and its precursors from continental regions upwind (Hudman et al., 2004; Derwent et al., 2004; Parrish et al., 2010). These studies have inferred contributions of between 2 and 10 ppbv to surface ozone in Western Europe and western N America from ozone precursor emissions in N America and Asia, respectively. European emissions also impact surface ozone in SE Asia by 0.2 to 3.5 ppbv (Duncan and Bey, 2004; Fiore et al., 2009; Wild et al., 2004), however export of European emissions eastwards is somewhat less efficient compared with N American and Asian pollution export. This is due to a paucity of strong cyclogenisis and frontal activity over Central and Eastern Europe compared with that over the N American and Asian east coasts (Stohl, 2001). Inter-continental transport contributions can lead to exceedences of regional air quality standards for ozone, and may become significant in the context of threshold parameters such as AOT40. As European and N American ozone precursor emissions continue to decline, rising East Asian emissions may play an increasing role in controlling NH background ozone (Cooper et al., 2010; Jacob et al., 1999), which has seen increases over the past 30 yr (Cooper et al., 2010; Derwent et al., 2004). Intercontinental contributions to crop ozone exposure and yield reductions have not yet been quantified, but are important to understand in the context of expected future changes in ozone precursor emissions in the Northern Hemisphere and other environmental threats to food security.

There have been a large number of field studies carried out to assess the response of crops to ozone exposure, especially in N America and Europe, and to a lesser extent in South and East Asia (Emberson et al., 2009). Mills et al. (2007) describe two major studies of note. These are the US National Crop Loss Assessment Network (NCLAN) studies conducted in the 1980s (Heagle, 1989) and the European Open Top Chamber Programme (EOTCP) conducted in the late 1980s and early 1990s (Jager et al., 1992). These studies aimed to establish the response of crop exposure to ozone and the resultant losses in yield. Mills et al. (2007) review a large set of crop ozone-response data from a number of sources in the existing literature (including data from the above coordinated field experiments) in order to derive exposure-response functions in terms of AOT40, M7 and M12 exposure indices, for a set of 19 European agricultural and horticultural crops.

Recent studies (Deb Roy et al., 2009; Tong et al., 2009b; Van Dingenen et al., 2009) have employed these indices to assess the exposure of crops to ozone over various regions of the world using atmospheric models to provide the necessary regional or global ozone concentration fields for the analysis. Van Dingenen et al. (2009) estimate the global impact of surface ozone on four major agricultural crops (wheat, rice, soy and maize) under current and future emission scenarios, focusing in particular on the impact of relative yield losses on production losses and resultant economic impacts. Van Dingenen et al. (2009) estimated that present day yield losses lie in the range of 7 % and 12 % for wheat, between 6 % and 16 % for soybean, between 3 % and 4 % for rice and between 3 % and 5 % for maize and that by 2030 (under a current legislation scenario) the global situation is expected to deteriorate mainly for wheat (additional

2–6 % loss globally) and rice (additional 1–2 % loss globally). They also estimate that using 2000 world market prices, the total global economic cost would be in the range of $14 to $26 billion.

These studies aim to provide quantification of ozone damage to crops on a global, regional and national scale, providing an indication of the resultant yield losses and economic impact. However, to our knowledge, no previous study has attempted to estimate the impact of ozone precursor emissions from each of the Northern Hemispheres major industrialized regions (N America, SE Asia, and Europe) on crop yields globally and in continents downwind.

In this study, we use a global chemical transport model to quantify the intercontinental contributions to ozone-induced crop yield reductions, due to anthropogenic NO_x emissions from the 3 major regions described above. We compare a control simulation for 2000 (standard model NO_x emissions) with 3 different emissions scenarios where a 100 % reduction is applied to anthropogenic NO_x emissions in each of the 3 regions separately. We use these scenarios to quantify contributions to regional crop yield reductions of six major crop types, from emission reductions in each region, using both AOT40 and Mx indices.

2 Methodology

2.1 TOMCAT Chemical Transport Model (CTM) and emissions scenarios

The global offline 3-D TOMCAT CTM (Arnold et al., 2005; Chipperfield, 2006) is used to simulate global tropospheric ozone for the year 2000 under the control and each of the 3 emissions reduction scenarios. TOMCAT is forced using meteorological data from the European Centre for Medium Range Weather Forecasts (ECMWF), at a horizontal resolution of ~2.8° with 31 vertical levels from the surface to 10 hPa. Sub-grid transport from convection (Stockwell and Chipperfield, 1999) and boundary layer turbulence (Holstag and Boville, 1993) is parameterized.

Tropospheric chemistry includes methane-NO_x-VOC-isoprene photochemistry, wet and dry deposition (Giannakopoulos et al., 1999), and NO_x emissions from lightning (Stockwell et al., 1999). The current dry deposition scheme accounts for 37 tracer species, including ozone.

A control simulation was used to calculate one year of hourly surface ozone for 2000 using IPCC AR5 “2000” anthropogenic emissions (Lamarque et al., 2010), Global Fire Emissions Database version 2 (GFED 2) biomass burning emissions climatology (van der Werf et al., 2006), in addition to POET biogenic emissions, used as described in (Emmons et al., 2010). In order to assess the contribution of NO_x emissions from the Northern Hemispheres major industrialized regions (N America, SE Asia, and Europe) to crop damage due to ozone exposure we define domains of the three regions as shown in Figure 1 and repeat simulations for 2000 with the following emission changes.

1. NA_EMSCUT: as control scenario, with a 100 % reduction in fossil fuel NO_x emissions over the North American domain.
2. SEA_EMSCUT: as control scenario, with a 100 % reduction in fossil fuel NO_x emissions over the South East Asian domain.
3. EUR_EMSCUT: as control scenario, with a 100 % reduction in fossil fuel NO_x emissions over the European domain.

We apply complete cuts in regional anthropogenic NO_x sources, to derive the signal of exposure contributions from the different regions, which may not be scalable linearly to smaller emission reductions when using threshold indices such as AOT40. The application of complete emissions cuts to each receptor region also allows us to quantify which regions anthropogenic NO_x emissions contribute the most to global ozone-induced yield losses. Details of NO_x emission totals for the regions under the control scenario are shown in Table 1. Hourly ozone concentrations were output from the midpoint of the lowest model layer, which is ~30 m above the surface. To account for the concentration gradient of ozone in the lowest model layer (produced by deposition to the surface), we scaled the model ozone to crop canopy height (assumed to be 1 m), using the approach of the (LRTAPConvention, 2004), as described by (Tuovinen et al., 2007).

2.2 Calculation of ozone exposure metrics and relative yield loss

Calculations of the Mx and AOT40 exposure indices are made using modeled hourly ozone (scaled to crop canopy height). Using AOT40, we calculate the relative yield loss for 6 major agricultural crops (wheat, rice, maize, soybean, cotton and potato) that are widely grown throughout the world. We use Mx to calculate relative yield loss for 4 of the crops (wheat, rice, maize and soybean). AOT40 is calculated during daylight hours when clear sky radiation is above 50 $\mathrm{W m^{-2}}$, values are accumulated over a predefined 3 month growing season which we define as May to July in the NH (offset by 6 months for SH locations). This growing season is chosen as within the NH the 6 crops investigated in this study have growing seasons that on average fall around this time period as highlighted during previous studies (Van Dingenen et al., 2009; Wang and Mauzerall, 2004). Defining a single crop growth window enables more comparability between the effects of the emissions reductions and the subsequent impact on ozone-induced yield losses for each of the crops. For the calculation of Mx we calculate the seasonal 7 h and 12 h daytime mean ozone over the duration of the same growing season used for AOT40. We follow the approach of previous studies (Deb Roy et al., 2009; Van Dingenen et al., 2009) and define daylight hours as a fixed 12-h period running from 08:00 to 19:59 LT for the calculation of AOT40 and M12. For M7 we use a 7-h time period of 09:00 to 15:59 LT.

Relative yield for each crop is calculated based on the exposure-response relationships compiled by Mills et al. (2007), which give linear exposure-response relationships as a function of AOT40 for all 6 of the crops that we have chosen for this study. Using AOT40 therefore allows us to consistently assess the impact of ozone exposure on both ozone sensitive (wheat, soybean and cotton) and moderately ozone tolerant (rice, maize and potato) crop types. The AOT40 exposure-response relationships for the 6 crops considered are shown in Table 2.

The AOT40 exposure-response relationships tend to have an intercept that is not equal to 1. In the case of some crops this can produce an offset that is high compared to the slope of the exposure-response relationship. Therefore we have adopted a similar approach to that used in Van Dingenen et al. (2009) and scaled the exposure response functions to their value at AOT40 = 0 such that the intercept of the relative yield is equal to 1. In order to calculate relative yield loss for wheat, rice maize and soybean using Mx we use the exposure response relationships from Wang and Mauzerall (2004) shown in Table 3.

One important aspect of the AOT40 relationships is that they only consider the effect of ozone damage when the ambient concentration is over 40 ppbv for a given hour. Ozone exposure below this threshold can still cause plant damage, as ozone can directly damage cells around leaf stomata and thus affect their ability to open and close (Ashmore, 2005; Sitch et al., 2007). It should also be considered that the AOT40 index was designed to capture the most harmful effects from episodic ozone pollution, however now that background levels of ozone are increasing (Cooper et al., 2010; Derwent et al., 2004) these threshold indices are starting to become less useful. A more accurate approach is to develop plant response relationships that are based around the flux of ozone into the plant. However, at present flux-response relationships are only available for wheat and potato (Pleijel et al., 2004) and have not been parameterised for global application. Hence we are unable to consider flux-response relationships in this study, however, we note that could be problems associated with suitability of these concentration based indices for application in regions different from those in which they were developed (Emberson et al., 2009). An aim of our analysis is to determine how use of these different metrics impacts our conclusions regarding transboundary yield loss contributions.

2.3 Crop distribution maps

We determine the distributions of the six crops using harvested area and yield data from the Center for Sustainability and the Global Environment (SAGE) at the University of Wisconsin (Monfreda et al., 2008). These datasets provide harvested area and yield for 175 distinct crops of the world on an approximately 10 km by 10 km (5 min resolution) latitude-longitude grid and are produced by combining national, state and county level census statistics from 206 countries, with a global data set of croplands. The data are regridded to the $\sim 2.8 \times 2.8^{\circ}$ TOMCAT horizontal resolution to provide maps of crop location for the calculation of crop-specific relative yield losses based upon the model-calculated AOT40 and Mx indices. Global maps of the crop locations are shown in Fig. 1.

We calculate AOT40 and Mx on a global scale over the defined growing season and then use the crop data to quantify regionally-aggregated yield losses (mean yield loss weighted according to area harvested and crop yield within each region) for each of the six major crops on a global scale and over each of the 3 considered NH regions.

3 Results

3.1 Comparison of model ozone concentrations and metrics with observational data

Figure 2 shows a comparison between observed and modeled monthly mean ozone concentrations from the year 2000 control simulation for regions considered in the study. For these comparisons, the model ozone at 30 m (the mid-point of the lowest model layer) was scaled using the approach of the LRTAP convention (2004) to a height of 10 m, the height at which most of the observational data is sampled.

Hourly observed ozone is averaged over several sites within each region, and is mainly taken from continuous ground based UV absorption based measurements. We make use of data from the European Monitoring and Evaluation Programme (EMEP), the USEPA and the World data centre for Greenhouse Gases (WDCGG) and have selected the sites from varying locations including both urban and rural locations as well as both coastal and inland locations, in order to provide coverage from polluted and relatively clean air locations. We have used sites from Japan and Malaysia for the comparison over Asia, as these sites provided the best continuous surface level ozone on a monthly basis. Hourly model output is taken from grid boxes containing each observation site position, before being averaged across sites within each region. Table 4, provides a summary of the regions compared as well as information on the sources of the observations.

Over the Mediterranean region and central Europe, the normalized model mean bias in surface ozone compared with observations is 5.3 % and −0.6 %, respectively. The model also performs well over SW USA where the model mean bias is −10.4 %. Over these regions the model ozone falls within one standard deviation of the observations for the majority of the year, particularly through the months of the growing season. Over the SE USA and SE Asia, the model mean bias exceeds 20 % in both locations, with modelled summer ozone seen to over-estimate observed surface ozone throughout the summer months. However over both regions the model falls within one standard deviation of the observations during the majority of the pre-defined growing season (May, June, and July), the only exception being July over SE Asia. During the winter months however, the model reproduces SE Asia surface ozone well, with model ozone falling within one standard deviation of the observation data. Over the Great Lakes region, the model tends to perform better with a model mean bias of 11.7 %, however summer ozone is over-estimated. Mean model surface ozone is seen to peak above the 40 ppbv threshold limit of AOT40, over SW USA, Mediterranean and Central Europe during the summer months and over the Great Lakes and SE USA during the spring, which coincides with the defined growing season for crops in the NH. Over SE Asia, a less distinct seasonal surface ozone cycle is seen due to the majority of the region lying within the tropical latitudes, where seasonality in insolation and its impacts on photochemistry are less pronounced. The positive model bias over SE Asia during the summer months could also be linked to the model inaccurately representing the monsoon period over SE Asia which typically runs from July to October. The monsoon season over SE Asia brings the transport of marine air masses and sees weak photochemical activity resulting in lower ozone concentrations than pre monsoon levels (Zhao et al., 2010).

Model ozone was also evaluated in terms of monthly averaged daylight hours (08:00 to 19:59 which also acts as monthly averaged M12) along with monthly accumulated AOT40. Figures 3 (M12) and 4 (AOT40) show the results of these comparisons with the same regions used as in Fig. 2, with the exception of SE Asia which has been replaced with Japan, since this is the only location in the region with continuous ozone data on an hourly basis.

Figure 3 shows good agreement between the model and measurements for M12 over SE USA, the Mediterranean and Central Europe with the model falling within one standard deviation of the observations for the majority of the year. One particular region to note is SE USA, which sees a large improvement in agreement between the model and observed M12 compared to the comparison with measured monthly mean ozone. This indicates that the model over-predicts nighttime ozone. This may be linked to the model failing to accurately decouple the shallow nighttime continental boundary layer, and mixing down ozone rich air from the free troposphere leading to a positive model bias on the monthly mean. For SW USA there is good agreement, however the model tends to under-predict the observed M12, particularly through the spring where modelled ozone is about 5–10 ppbv lower than measured M12.

For the Great lakes and SE Asia, model M12 falls within one standard deviation of the observations, with the exception of throughout July over the Great lakes. Overall however, the model tends to over predict summer M12 and under predict springtime M12.

For AOT40, the model shows the best agreement over SW USA, SE USA and the Mediterranean (Fig. 4). Overall, it can be seen that during the growing season the

Title Page
Abstract Introduction
Conclusions References
Tables Figures
◀| |▶
◀ ▶
Back Close
Full Screen / Esc
Printer-friendly Version
Interactive Discussion

model reproduces the observed AOT40 within one standard deviation for most regions, with the exception of the Great Lakes in July (positive model bias) and Central Europe in May and June (negative model bias).

Figures 3 and 4 also show the regional normalized model mean biases for AOT40 and M12. For M12, the model bias to observed M12 is between −13.3 % and 4 %. For AOT40, the model bias lies between −65.2 % and 60.4 %. While larger than biases for M12, these are comparable to model biases found in the recent global ozone crop exposure study of Van Dingenen et al. (2009). This indicates that from a modelling perspective, AOT40 may be a less robust metric for assessing crop exposure to ozone than the concentration average Mx indices. This agrees with the findings of Tuovinen et al. (2007).

3.2 AOT40 and Mx changes under emissions reductions scenarios

Figure 5 shows global plots of the relative differences in AOT40 between the control and each of the emissions reduction scenarios, along with global AOT40 calculated for the 3 month growing season (May, June and July for the NH, offset by 6 months for the SH) for control NO_x emissions. The AOT40 index is particularly large over the major industrialized regions with peak AOT40 values approaching 20 ppm h over the eastern seaboard of the United States as well as over eastern China and the Middle East.

Local NO_x emission cuts result in a near 100 % relative decrease in AOT40 over each of the regions, although reductions over SE Asia are smaller (87.8 %). The effect of NO_x emissions from each of the regions on AOT40 in downstream receptor locations is also evident. A 100 % reduction in N American anthropogenic NO_x emissions results in mean relative decreases in AOT40 over the European region of 50.1 %, with decreases approaching 60 % over parts of north and western Europe. This transboundary effect extends into SE Asia with mean relative decreases in AOT40 of ∼14 % and greatest reductions in AOT40 over western and northern parts of the region. A 100 % reduction in SE Asian NO_x emissions results in ∼22 % reduction in AOT40 over

N America with greatest decreases in AOT40 seen over the western seaboard of the US and parts of Canada and Greenland where reductions in AOT40 approach 60 %. A smaller impact is seen over the European region, where mean reductions in AOT40 are approximately 3 %. The impact of a 100 % reduction in European NO_x emissions on AOT40 is approximately the same over N America and SE Asia. Over SE Asia, mean regional relative decreases in AOT40 are ∼14 % with greatest reductions seen over parts of north western China and western Mongolia. The impact on N American AOT40 is ∼15 %, with reductions in AOT40 observed to approach 40 % over the west coast of the continental United States. Overall, reductions in NO_x emissions over N America produce the largest overall global impact on AOT40, with N American NO_x also producing the largest transboundary effect, shown by a mean reduction of 50.1 % in AOT40 over Europe under a 100 % emissions cut. Additional calculations suggest that the relative importance of NO_x emission reductions from each of the regions in reducing AOT exposure is invariant when the threshold of the AOT index is varied from 30 to 60 ppbv (see Supplement).

Figures 6 and 7 show respectively M7 and M12 seasonal mean ozone concentrations under the control scenario calculated over the same growing season as for AOT40, as well as differences resulting from the three emission reduction scenarios. NO_x emission reductions over each of the regions result in local reductions of M7 and M12 of 20 % or greater. Overall however, the transboundary impacts of NO_x emission reductions on Mx are less pronounced than the impact on AOT40. A 100 % reduction in N American NO_x results in relative decreases in Mx of around 7.3 % over Europe, with greatest reductions over north and western parts. The impact on SE Asia is much less with reductions in Mx for the region of around 1.2 %. A 100 % reduction in SE Asian NO_x emissions, results in relative decreases of around 2.4 % in Mx over the N American region with the biggest reductions over western continental United States and Canada. The impact of SE Asian emissions cuts on Europe is small with reduction in Mx over the region of less than 1 %. Similar to AOT40, NO_x emissions reductions over Europe tend to produce approximately similar reductions in Mx over the N American and SE

Asian receptor regions with mean regional relative decreases in Mx slightly larger over N America (~2.0 %) than over SE Asia (~1.3 %).

Overall, reductions in NO_x emissions produce a similar pattern in the global AOT40 and Mx fields with N American NO_x producing the largest global scale impact. N American emission reductions exhibit the largest transboundary effect, shown by the response of all 3 metrics over Europe to a 100 % cut in anthropogenic NO_x over N America.

3.3 Ozone induced relative yield losses for 2000 under the model control scenario

Table 5 shows regionally-aggregated ozone-induced relative yield losses for the control model scenario (based on both AOT40 and Mx for wheat, rice, maize and soybean and based on AOT40 for potato and cotton). On a global scale, wheat, soybean and cotton are the most sensitive of the crops. For wheat, the relative yield loss values range from 3.6 to 5.4 % with AOT40 giving the largest value. Relative yield losses for soybean range from 4.3 to 11.4 % with M12 giving the largest value. For cotton we only present yield losses based on AOT40, which show a global value of 6.8 %. Rice and maize demonstrate higher tolerance to ozone exposure, with yield losses of around 1.0 % (for both AOT40 and M7) for rice and 1.5 to 3.6 % for maize. Potato yield losses are 1.4 % globally, based upon AOT40.

Table 5 also shows the regionally-aggregated relative yield losses for the three individual regions. For rice and soybean, relative losses tend to be highest over N America (up to 15.3 % for soybean and 1.7 % for rice). For wheat, maize and potato the relative losses are largest over SE Asia with losses of up to 10.5 % for wheat, 3.0 % for potato, and 4.7 % for maize Finally for cotton, highest yield losses are seen over N America and SE Asia with relative yield loss values slightly higher over SE Asia at 8.5 % compared to 8.1 % over N America. These regional relative yield losses partly reflect the geographical locations of the crops, but also the amount of yield produced for each crop over each region, and locations of elevated ozone. As such, they highlight locations where particular crops are most sensitive to present-day ozone exposure and which regions are most at risk of suffering economic loss through ozone-induced crop yield reduction.

A comparison with a previous similar study (Van Dingenen et al., 2009) shows our results produce a similar pattern of global relative yield losses for wheat, rice, maize and soybean (cotton and potato are not considered in Van Dingenen et al., 2009) with wheat and soybean being the most sensitive crops to ozone exposure. Van Dingenen et al. (2009) also demonstrate largest relative yield losses produced from AOT40 values for wheat, and M12 producing the largest relative yield losses for soybean. Our yield loss values for wheat (3.6 to 5.4 %) and soybean (4.3 to 11.4 %) are smaller than those shown in Van Dingenen et al. (2009) which are 7.3 to 12.3 % for wheat and 5.4 to 15.6 % for soybean. The relative yield losses for rice and maize (1.0 % and 1.5 % to 3.6 %, respectively) are also smaller here than those of Van Dingenen et al. (2009) (2.8 to 3.7 % for rice and 2.4 to 4.1 % for maize). Differences between our results and those of Van Dingenen et al. (2009) can be explained by the use of different crop distribution maps to identify crop locations and yields, as well as different definition of growing seasons for each of the crops. These factors result in different exposure of crops to ozone and hence different relative yield loss values under the control scenario. In addition, the surface ozone distributions produced from the different CTMs used are likely somewhat different. Nevertheless, our control scenario produces comparable magnitudes of yield losses to those described by Van Dingenen et al. (2009), and transboundary effects highlighted under our emission reductions scenarios are based upon control yield losses that are similar in magnitude and distribution.

3.4 Impact of regional cuts in NO_x emissions on ozone induced relative yield losses

The impact of regional reductions in NO_x emissions on regionally-aggregated ozone-induced yield loss calculated from AOT40 exposure is shown in Fig. 8 for six crop types. Globally, N American NO_x emission reductions result in largest changes to yield loss

Title Page
Abstract | Introduction
Conclusions | References
Tables | Figures
◀| |▶
◀ ▶
Back | Close
Full Screen / Esc
Printer-friendly Version
Interactive Discussion

for soybean and maize. SE Asian NO_x emission reductions result in largest changes to wheat, rice, cotton and potato yield loss. This primarily reflects the geographical distributions of these six crops and their yield distributions. For each of the six crops, local reductions in NO_x emissions result in near 100 % reduction in ozone-induced relative yield loss over each of the regions, demonstrating that according to the AOT40 exposure metric, local emission controls and air pollution strategies could effectively mitigate ozone-induced yield losses. However, ozone-related yield losses for rice and potato grown in N America cannot be completely eliminated through local emissions reductions.

In the European region, yield losses are reduced by at least 39 % when cutting N American NO_x emissions. Rice yield loss shows the most sensitivity to N American emissions (55.6 %) with cotton showing the greatest sensitivity to SE Asian NO_x sources (12.0 %). Potato shows the lowest sensitivity to both N American (39.2 %) emissions and SE Asian (1.22 %) emissions. When diagnosed with AOT40, the impacts of N American emissions on European yield loss are the largest intercontinental transboundary effect in this study. The minimum 39.2 % reduction in European potato yield loss from N American emission cuts is larger than both the maximum European emission impact on SE Asia yields (10.4 % for cotton) and the SE Asian emission impact on N American yields (34.9 % for potato). Over N America, the largest non-local impact on relative yield loss results from SE Asian NO_x, with yield loss reductions ranging from 34.9 % for potato to 4.67 % for soybean. N American yield loss reductions of 1.27–9.57 % result from reductions in European NO_x, with potato and wheat showing the largest sensitivities. On the whole, yield losses of all six crops over SE Asia are reduced by approximately equal amounts as a result of N American and European emissions reductions, with N American NO_x cuts producing slightly higher yield loss reductions for wheat, maize and soybean and European NO_x cuts producing slightly higher yield loss reductions for rice, cotton and potato. Cotton yield losses show the greatest difference, with European emissions cuts producing a reduction in yield of 10.4 % compared with a reduction of 9.6 % produced by N American emissions cuts.

Figure 9 shows the impact of regional reductions in NO_x emissions for 4 of the 6 crop types considered (using the M7 index for wheat and rice and the M12 index for maize and soybean), on both a global scale and in each of the receptor regions.

Globally, N American NO_x emission reductions dominate maize and soybean yield loss reductions and SE Asian NO_x emissions reductions dominate wheat and rice yield loss reductions, again primarily reflecting the geographical distributions of the crops.

For all 4 crops, local reductions in NO_x emissions result in between an 87.2 % reduction in soybean yield losses over SE Asia to a 98.3 % reduction in soybean yield losses over N America. This shows that under the emissions reduction scenarios, the local yield loss reductions calculated from Mx tend to be less pronounced than those calculated from AOT40.

In the European region, a 100 % cut in N American NO_x emissions dominates yield loss reductions with at least a 12.4 % reduction in relative yields observed under the N American emissions cuts. Using the Mx indices, the impact of N American NO_x emissions on European yields are the largest transboundary effect, as with AOT40. Rice yield losses show the most sensitivity to both N American NO_x sources (25.5 %) and SE Asian sources (2.23 %) and soybean shows the least sensitivity to both N American (12.4 %) and SE Asian (1.05 %) sources. Over N America, the greatest non-local impact on relative yield results from SE Asian NO_x, with yield loss reductions ranging from 9.18 % for wheat to 2.44 % for soybean. European NO_x sources contribute less to yield loss with reductions of 0.78–3.66 %, with maize and wheat showing the largest sensitivities. Overall, yield losses for SE Asia are reduced by approximately equal amounts as a result of cuts to N American and European NO_x with European emissions cuts producing slightly larger yield loss reductions. Maize yield losses show the greatest difference with European emissions cuts producing a reduction in yield of 5.18 % compared with a reduction of 4.85 % produced by N American emissions cuts.

4 Discussion

Using the 3 metrics (AOT40/M7/M12), model calculations show that for 4 of the major crops considered (wheat, rice, cotton and potato) reductions in SE Asian NO_x emissions tend to produce the greatest reduction in crop yield losses (48.8 to 94.7 %) on a global scale. Cuts to N American emissions result in the greatest global impact on crop yield reductions for maize and soybean (57.5 to 81.7 %). The changes in yield losses based on Mx show a similar pattern to those calculated using the AOT40 index, however they are less pronounced than the yield loss changes produced using AOT40. Figure 2 shows that under control emissions, modelled mean monthly surface ozone is slightly above the 40 ppbv threshold of AOT40, particularly over Europe, SW USA and SE Asia. Under emission reduction scenarios, small reductions in ozone resulting in concentrations falling below 40 ppbv can produce a relatively large decrease in AOT40. Due to the linear relationship of yield loss with AOT40, this produces a comparable relative change in yield. The change in Mx however, is directly related to the fractional change in mean background ozone, which may be smaller than the respective change in AOT40 where ozone is near to 40 ppbv. Due to the Weibull relationship between Mx and relative yield loss (Table 3), a given change in Mx also produces smaller changes in relative yield loss.

N American NO_x emissions produce the largest intercontinental ozone impact in this study. This is consistent with previous studies that have shown trans-Atlantic transport of ozone to be more efficient compared with trans-Pacific and trans-Siberian transport (Stohl, 2001). European NO_x emissions tend to produce a greater local impact on crops rather than a transboundary impact, as the export of ozone and its precursors from the European domain is less efficient than from the other regions, due to less frontal lifting over Eastern Europe (Stohl, 2001), and because of the more northerly latitudes of Europe compared with the other two regions.

The results demonstrate that local air quality and emissions control strategies over each of the regions have the potential to effectively mitigate ozone-induced yield losses for six major crop types. A 100 % reduction in local anthropogenic NO_x emissions results in near 100 % reductions in AOT-40 derived crop yield losses for wheat, rice, maize, soybean, cotton and potato in each of the regions.

However, in N America, a 100 % reduction in local NO_x produces an 89.5 % reduction in local rice yield losses and an 88.5 % reduction in potato yield losses. This indicates a smaller sensitivity of 40 ppbv exeedences over potato and rice growing regions to local anthropogenic emissions compared to Europe and SE Asia. It can be seen from Fig. 1 that over the N American region the majority of Potato growing regions are over north and western parts of the region. The crop yield data (see Supplement) also indicates that the greatest potato yields are seen to the north west of the N American region. With respect to rice, Fig. 1 shows little rice growing over the region with some rice grown over the south east and a small area along the west coast. The yield data however again shows higher yields of rice to the West of the N American region. In a recent study (Jaffe, 2011) it is shown that for the period 1995–2009, biomass burning emissions through the summer are significantly correlated with the number of days where surface ozone exceeds guideline levels in the western United States. This indicates that biomass burning emissions could be playing a role in controlling the exposure of crops to ozone in this region. Since the emission cuts are only shutting off anthropogenic NO_x the impact of biomass burning emissions could still lead to exceedances of the 40ppbv threshold of AOT40.

As discussed above, the threshold nature of the AOT40 index means that it is sensitive to small ozone concentration changes around 40 ppbv. Contributions of a few ppbv to surface ozone from non-local emissions therefore have the potential to significantly alter the AOT40 exposure of crops in these regions. This also results in a large sensitivity to errors in the model surface ozone distribution, and consequent uncertainty in the AOT40-derived yield losses (Tuovinen et al., 2007). The present-day sensitivities of AOT40-derived yield loss to non-local emissions are a function of not only the non-local ozone precursor emissions themselves, but also the local ozone abundance. In more general terms, the threshold nature of the AOT40 metric results in long-range transport contributions to yield loss being strongly dependent on local ozone concentrations. Figure 10 shows calculations of the change in AOT40 as a function of mean local ozone concentration and the ozone contribution from long-range transport, assuming a normal distribution of local ozone concentrations. Maximum sensitivity of AOT40 to non-local ozone is seen where the mean local ozone is close to 40 ppbv. In addition, a relatively small variability in local ozone around 40 ppbv increases this sensitivity. This highlights the problem of using a threshold metric to assess contributions of different ozone sources to local yield loss. Under future emission and climate scenarios, where surface ozone concentrations may be larger in many regions, the AOT40-derived yield-loss response to non-local emission reductions may reduce, if such reductions are not sufficient to bring ozone concentrations below the 40 ppbv threshold. Alternatively, under a scenario where local emissions in Europe and N America are reduced, but an increase in background ozone concentrations is driven by increasing Asian emissions (e.g. Jacob et al., 1999), the sensitivity of European and N American AOT40 yield-loss to Asian emission reductions may increase.

Since relative yield loss is linearly related to AOT40 (Mills et al., 2007), the reduction in yield loss under the emissions cut scenarios changes proportionally with the magnitude of a change in AOT40. Assuming under each of the emission scenarios ozone remains greater than 40 ppbv, this leads to a linear relationship between ozone reduction and yield loss reduction, which is independent of the absolute ozone concentration. For the concentration based indices Mx, yield loss reductions depend on the magnitude of the absolute ozone concentration, in addition to the ozone change. This is due to the non-linear Weibull relationship between yield loss and Mx (shown in Fig. 11), which is also dependent on the sensitivity of each crop to ozone exposure. With the exception of soybean, at larger values of Mx, a given change in the mean background ozone concentration would result in a greater response of yield reduction for each crop, than at smaller Mx. At lower background levels of ozone the response of yield to a given change in ozone is much less. This behaviour means that the Mx indices can become close to mimicking a threshold response, similar to that of AOT40.

Title Page
Abstract Introduction
Conclusions References
Tables Figures
◀| |▶
◀ ▶
Back Close
Full Screen / Esc
Printer-friendly Version
Interactive Discussion

This behaviour also means that under increased background ozone, the relative yield loss changes produced under the respective emissions cut scenarios would be more pronounced.

The results of this study only consider crop yield losses that are related to ozone exposure. In reality, there are many other drivers that can cause a reduction in crop yields. These factors include exposure to higher temperatures under a warmer climate, drought stress, and whether the crops are properly irrigated. It is shown in (Liu et al., 2010), that for a winter wheat-summer maize cropping system in the Huang-Huai-Hai Plain of China, a 5 °C increase in temperature results in an overall yield reduction of −18.5 ± 22.8 %. They also present an overall yield reduction of −2.3 ± 13.2 % for temperature rise of 2 °C.

By comparison, the results presented here show that for the SE Asia receptor region (which contains China), for wheat, regionally-aggregated relative yield losses due to ozone exposure are 5.4 to 10.5 % (Table 5), showing that ozone-induced crop damage under control emissions for 2000 is greater than that caused by 2 °C temperature rise and roughly half of that of a 5 °C temperature rise. For maize, the effect of ozone damage over SE Asia is less with relative yield losses of 2.3 to 4.7 %. An additional factor to consider is the possible benefits to crop yields under future climate due to fertilization from enhanced CO_2, which can act to increase the biomass of crops (Franzaring et al., 2008) and potentially increase crop yields. This could offset yield losses through rising ozone or temperatures. The location of crop cultivation, the extent of crop irrigation and the management of the crops are also important factors to consider. It has also been shown in a recent study that ozone damage to plants can feed back on yield loss through the effect on evapotranspiration. Bernacchi et al. (2011) showed that ozone exposure of soybean can reduce water use by as much as 15 %, resulting in increased sensible heat flux which is indicative of a day-time increase in canopy temperature of up to 0.7 °C, with warmer temperatures leading to further reduction in crop yields (Liu et al., 2010). With a rise in surface ozone coupled with a warmer climate, the ozone-induced yield loss may act to enhance the yield loss observed for crops due to the warmer temperatures, however it should be noted that these yield-limiting factors interact in non-linear ways depending on whether warmer temperatures limit ozone uptake and hence the damage caused. The transboundary impact of ozone and its precursor emissions on yields highlight that even non-local emission reduction strategies could at least partially offset a reduction in crop yields under a warmer future climate. These feedbacks all play important roles in how climate change and emission changes may affect crop yields.

5 Conclusions

This study is the first to estimate the impact of ozone precursor emissions from each of the Northern Hemispheres major industrialized regions (N America, SE Asia, and Europe) on crop yields globally and in continents downwind, and is the first to attempt to use a range of available indices applied in a standardized manner to assess the potential impact of intercontinental transboundary pollution on crop yields.

We have shown that for 4 of the crops considered (wheat, rice, cotton and potato), model calculations estimate that reductions in SE Asian NO_x emissions tend to produce the greatest reduction in crop yield losses (48.8 to 94.7 %) when based on AOT40/Mx, on a global scale. Cuts to N American emissions result in the greatest global impact on crop yield reductions for maize and soybean (57.5 to 81.7 %). It is also shown that NO_x emissions from N America exhibit the largest non-local effect, resulting in European yield loss reductions of between 12.4 % and 55.6 %, when a 100 % cut is applied to NO_x emissions from the N American region. This demonstrates that local air quality and emission control strategies have the potential to partly alleviate ozone-induced crop yield loss in continents downstream, in addition to effectively mitigating local ozone-induced yield losses.

It is important to consider however that these indices have not been designed with the specific purposes of estimating yield losses due to the intercontinental transport of ozone. The exposure response functions used are based on data collected from cultivars of crops grown in N America and Europe. It has been highlighted in a recent study (Emberson et al., 2009) that crops grown in Asia, particularly wheat and rice, may be more sensitive to ozone exposure than these relationships may suggest. These indices were also developed in regions where, at the time, concern was placed on peak ozone concentrations (Heck and Colwing, 1997). Since their development, regional ozone distributions have changed, due to declining ozone precursor emissions over N America and Europe, and due to rising emissions over East Asia playing a more important role in background NH ozone (Cooper et al., 2010; Jacob et al., 1999). This shift has resulted in less episodic high ozone events, but an increase in the background ozone concentrations over Europe and N America. This may result in different exposure regimes of crops to ozone and hence the resultant impact on yield loss.

This study could be extended to incorporate flux-response relationships to assess the effect of long range transport of ozone and its precursors on crops. Flux based methods consider the flux of ozone into the plant, mainly through the stomata, and can begin to account modifying environmental conditions and hence could be more applicable in different global regions and future climates (Harmens et al., 2007). These relationships also allow for variable concentration based thresholds as appropriate to where the plants are grown and the conditions in which they are cultivated. However, at present flux-response relationships are only available for wheat and potato (Pleijel et al., 2004), and these have not been parameterized for global application.

Supplementary material related to this article is available online at: http://www.biogeosciences-discuss.net/8/8645/2011/ bgd-8-8645-2011-supplement.pdf.

Acknowledgements. The authors wish to acknowledge the World data centre for Greenhouse Gases (WDCGG), the Japanese Meteorological Agency, BMKG and EMPA for provision of model validation data over SE Asia as well as the EMEP and CASTNET networks for providing model validation data over Europe and N America, respectively. This work was supported with funding from the UK Natural Environment Research Council (NERC).

References

Adams, R., Crocker, T., and Thanavibulchai, N.: An economic assessment of air pollution damages to selected annual crops in southern California, J. Environ. Econ. Manag., 9, 42–58, 1982. 8647

Arnold, S., Chipperfield, M., and Blitz, M.: A three-dimensional model study of the effect of new temperature-dependent quantum yields for acetone photolysis, Geophys. Res.-Atmos., 110, D22305, doi:10.1029/2005JD005998, 2005. 8651

Ashmore, M.: Assessing the future global impacts of ozone on vegetation, Plant Cell Environ., 28, 949–964, 2005. 8648, 8654

Aunan, K., Bernsten, T., and Seip, H.: Surface Ozone in China and its possible impact on agricultural crop yields, Ambio, 29, 294–301, 2000. 8647

Bernacchi, C., Leakey, A., Kimball, B., and Ort, D.: Growth of soybean at future tropospheric ozone concentrations decreases canopy evapotranspiration and soil water depletion, Environ. Pollut., 159, 1464–1472, 2011. 8667

Chipperfield, M. P.: New version of the TOMCAT/SLIMCAT off-line chemical transport model: Intercomparison of stratospheric tracer experiments, Q. J. Roy. Meteorol. Soc., 132, 1179–1203, 2006. 8651

Cooper, O. R., Parrish, D. D., Stohl, A., Trainer, M., Nedelec, P., Thouret, V., Cammas, J. P., Oltmans, S. J., Johnson, B. J., Tarasick, D., Leblanc, T., McDermid, I. S., Jaffe, D., Gao, R., Stith, J., Ryerson, T., Aikin, K., Campos, T., Weinheimer, A., and Avery, M. A.: Increasing springtime ozone mixing ratios in the free troposphere over western North America, Nature, 463, 344–348, 2010. 8650, 8654, 8669

Crutzen, P., Lawrence, M., and Pöschl, U.: On the background photochemistry of tropospheric ozone, Tellus A, 51, 123–146, 1999. 8647

Deb Roy, S., Beig, G., and Ghude, Sachin D.: Exposure-plant response of ambient ozone over the tropical Indian region, Atmos. Chem. Phys., 9, 5253–5260, doi:10.5194/acp-9-5253-2009, 2009. 8650, 8653

Derwent, R., Stevenson, D., Collins, W., and Johnson, C.: Intercontinental transport and the origins of the ozone observed at surface sites in Europe, Atmos. Environ., 38, 1891–1901, 2004. 8649, 8650, 8654

Duncan, B. and Bey, I.: A modeling study of the export pathways of pollution from Europe: Seasonal and interannual variations (1987–1997), J. Geophys. Res.-Atmos., 109, D08301, doi:10.1029/2003JD004079, 2004. 8649

EEA: Environmental assessment Report No. 2, Environment in the European Union at the turn of the century, European Environment Agency, Copenhagen, 446 pp., 1999. 8647

Emberson, L. D., Bueker, P., Ashmore, M. R., Mills, G., Jackson, L. S., Agrawal, M., Atikuzzaman, M. D., Cinderby, S., Engardt, M., Jamir, C., Kobayashi, K., Oanh, N. T. K., Quadir, Q. F., and Wahid, A.: A comparison of North American and Asian exposure-response data for ozone effects on crop yields, Atmos. Environ., 43, 1945–1953, 2009. 8650, 8654, 8669

Emmons, L. K., Walters, S., Hess, P. G., Lamarque, J.-F., Pfister, G. G., Fillmore, D., Granier, C., Guenther, A., Kinnison, D., Laepple, T., Orlando, J., Tie, X., Tyndall, G., Wiedinmyer, C., Baughcum, S. L., and Kloster, S.: Description and evaluation of the Model for Ozone and Related chemical Tracers, version 4 (MOZART-4), Geosci. Model Dev., 3, 43–67, doi:10.5194/gmd-3-43-2010, 2010. 8652

Fiore, A. M., Dentener, F. J., Wild, O., Cuvelier, C., Schultz, M. G., Hess, P., Textor, C., Schulz, M., Doherty, R. M., Horowitz, L. W., MacKenzie, I. A., Sanderson, M. G., Shindell, D. T., Stevenson, D. S., Szopa, S., Van Dingenen, R., Zeng, G., Atherton, C., Bergmann, D., Bey, I., Carmichael, G., Collins, W. J., Duncan, B. N., Faluvegi, G., Folberth, G., Gauss, M., Gong, S., Hauglustaine, D., Holloway, T., Isaksen, I. S. A., Jacob, D. J., Jonson, J. E., Kaminski, J. W., Keating, T. J., Lupu, A., Marmer, E., Montanaro, V., Park, R. J., Pitari, G., Pringle, K. J., Pyle, J. A., Schroeder, S., Vivanco, M. G., Wind, P., Wojcik, G., Wu, S., and Zuber, A.: Multimodel estimates of intercontinental source-receptor relationships for ozone pollution, J. Geophys. Res.-Atmos., 114, D04301, doi:10.1029/2008JD010816, 2009. 8649

Franzaring, J., Hoegy, P., and Fangmeier, A.: Effects of free-air CO_2 enrichment on the growth of summer oilseed rape (Brassica napus cv. Campino), Agr. Ecosyst. Environ., 128, 127–134, 2008. 8667

Fuhrer, J.: Ozone risk for crops and pastures in present and future climates, Naturwissenschaften, 96, 173–194, 2009. 8647

Fuhrer, J. and Achermann, B.: Critical Levels for Ozone: A UN-ECE Workshop Report, in: Critical Levels for Ozone: A UN-ECE Workshop Report, Liebefeld-Bern, Switzerland, Nr. 16, 1994. 8647

Giannakopoulos, C., Chipperfield, T. P., Law, K. S., and Pyle, J. A.: Validation and intercomparison of wet and dry deposition schemes using Pb-210 in a global three-dimensional off-line chemical transport model, J. Geophys. Res.-Atmos., 104, 23761–23784, 1999. 8652

Harmens, H., Mills, G., Emberson, L. D., and Ashmore, M. R.: Implications of climate change for the stomatal flux of ozone: A case study for winter wheat, Environ. Pollut., 146, 763–770, 2007. 8669

Heagle, A. S.: Ozone and Crop Yield, Annu. Rev. Phytopathol., 27, 397–423, 1989. 8650

Heck, W. and Colwing, E.: The need for a long term cumulative secondary ozone standard – an ecological perspective, Environmental Manager, January 1997. 8648, 8669

Heck, W., Cure, W., Rawlings, J., Zaragoza, L., Heagle, A., Heggestad, H., Kohut, R., Kress, L., and Temple, P.: Assessing Impacts Of Ozone On Agricultural Crops. 2. Crop Yield Functions And Alternative Exposure Statistics, JAPCA J. Air Waste Ma., 34, 810–817, 1984. 8649

Holland, M., Mills, G., Hayes, F., Buse, A., Emberson, L., Cambridge, H., Cinderby, S., Terry, A., and Ashmore, M.: Economic assessment of crop yield losses from ozone exposure. Report to UK Department of Environment, Food and Rural affairs under contract 1/2/170, Centre for Ecology and Hydrology, Bangor, 2002. 8647

Holstag, A. A. M. and Boville, B. A.: Local Versus Nonlocal Boundary-Layer Diffusion In A Global Climate Model, J. Climate, 6, 1825–1842, 1993. 8651

Hudman, R., Jacob, D., Cooper, O., Evans, M., Heald, C., Park, R., Fehsenfeld, F., Flocke, F., Holloway, J., Hubler, G., Kita, K., Koike, M., Kondo, Y., Neuman, A., Nowak, J., Oltmans, S., Parrish, D., Roberts, J., and Ryerson, T.: Ozone production in transpacific Asian pollution plumes and implications for ozone air quality in California, J. Geophys. Res.-Atmos., 109, D23S10, doi:10.1029/2004JD004974, 2004. 8649

Jacob, D., Logan, J., and Murti, P.: Effect of rising Asian emissions on surface ozone in the United States, Geophys. Res. Lett., 26, 2175–2178, 1999. 8650, 8666, 8669

Jaffe, D.: Relationship between Surface and Free Tropospheric Ozone in the Western US, Environ. Sci. Technol., 45, 432–438, 2011. 8665

Jager, H., Unsworth, M., De Temmerman, L., and Mathy, P.: Effects of Air Pollutants on Agricultural Crops in Europe, results of the European Open-Top Chambers project, in: Air Pollution Research Report No. 46, 46, 1992. 8650

Jager, H., Unsworth, M., De Temmerman, L., and Mathy, P.: Effects of Air Pollutants on Agricultural crops in Europe: results of the European Open-Top Chambers Project, Air Pollution Series of the Environmental Research Programme of the Commission of the European Communities, Directorate-General for Science, Research and Development, Brussels, Belgium, Report No. 46, 1996. 8647

Lamarque, J.-F., Bond, T. C., Eyring, V., Granier, C., Heil, A., Klimont, Z., Lee, D., Liousse, C., Mieville, A., Owen, B., Schultz, M. G., Shindell, D., Smith, S. J., Stehfest, E., Van Aardenne,

Title Page
Abstract Introduction
Conclusions References
Tables Figures
◂◂ ▸▸
◂ ▸
Back Close
Full Screen / Esc
Printer-friendly Version
Interactive Discussion

J., Cooper, O. R., Kainuma, M., Mahowald, N., McConnell, J. R., Naik, V., Riahi, K., and van Vuuren, D. P.: Historical (1850–2000) gridded anthropogenic and biomass burning emissions of reactive gases and aerosols: methodology and application, Atmos. Chem. Phys., 10, 7017–7039, doi:10.5194/acp-10-7017-2010, 2010. 8652

Li, X. S., He, Z. S., Fang, X. M., and Zhou, X. J.: Distribution of surface ozone concentration in the clean areas of China and its possible impact on crop yields, Adv. Atmos. Sci., 16, 154–158, 1999. 8647

Lin, C. Y. C., Jacob, D. J., and Fiore, A. M.: Trends in exceedances of the ozone air quality standard in the continental United States, 1980–1998, Atmos. Environ., 35, 3217–3228, 2001. 8649

Liu, S., Mo, X., Lin, Z., Xu, Y., Ji, J., Wen, G., and Richey, J.: Crop yield responses to climate change in the Huang-Huai-Hai Plain of China, Agr. Water Manage., 97, 1195–1209, 2010. 8667

LRTAPConvention: Manual on Methodologies and Criteria for Modelling and Mapping Critical Loads and Levels and Air Pollution Effects, Risks and Trends, International Cooperative Programme on Mapping and Modelling under the UNECE Convention on Long-Range-Transboundary Air Pollution, 2004. 8653

Mills, G., Buse, A., Gimeno, B., Bermejo, V., Holland, M., Emberson, L., and Pleijel, H.: A synthesis of AOT40-based response functions and critical levels of ozone for agricultural and horticultural crops, Atmos. Environ., 41, 2630–2643, 2007. 8650, 8653, 8666, 8677

Monfreda, C., Ramankutty, N., and Foley, J. A.: Farming the planet: 2. Geographic distribution of crop areas, yields, physiological types, and net primary production in the year 2000, Global Biogeochem. Cy., 22, GB1022, doi:10.1029/2007GB002947, 2008. 8655

Parrish, D. D., Aikin, K. C., Oltmans, S. J., Johnson, B. J., Ives, M., and Sweeny, C.: Impact of transported background ozone inflow on summertime air quality in a California ozone exceedance area, Atmos. Chem. Phys., 10, 10093–10109, doi:10.5194/acp-10-10093-2010, 2010. 8649

Pleijel, H., Danielsson, H., Ojanpera, K., De Temmerman, L., Hogy, P., Badiani, M., and Karlsson, P. E.: Relationships between ozone exposure and yield loss in European wheat and potato – a comparison of concentration- and flux-based exposure indices, Atmos. Environ., 38, 2259–2269, 2004. 8654, 8669

Prather, M., Ehhalt, D., Dentener, F., Derwent, R., Dlugokencky, E., Holland, E., Isaksen, I., Katima, J., Kirchhoff, V., Matson, P., Midgley, P., and M., W.: Climate Change 2001: The

Scientific Basis, chap. Atmospheric chemistry and greehouse gases, Cambridge University Press, New York, 239–287, 2001. 8647

RoyalSociety: Ground level ozone in the 21st Century: Future trends, impacts and policy implications., rS Policy Document 15/08, ISBN 978-0-85403-713-1, 2008. 8647

Sitch, S., Cox, P. M., Collins, W. J., and Huntingford, C.: Indirect radiative forcing of climate change through ozone effects on the land-carbon sink, Nature, 448, 791–794, 2007. 8648, 8654

Soldberg, S. and Lindskog, A.: The Development of European Surface Ozone. Implications for a Revised Abatement Policy, EMEP/CCC-Report 1/, 2005. 8649

Stockwell, D. Z. and Chipperfield, M. P.: A tropospheric chemical-transport model: Development and validation of the model transport schemes, Q. J. Roy. Meteorol. Soc., 125, 1747–1783, 1999. 8651

Stockwell, D. Z., Giannakopoulos, C., Plantevin, P. H., Carver, G. D., Chipperfield, M. P., Law, K. S., Pyle, Y. A., Shallcross, D. E., and Wang, K. Y.: Modelling NO_x from lightning and its impact on global chemical fields, Atmos. Environ., 33, 4477–4493, 1999. 8652

Stohl, A.: A 1-year Lagrangian "climatology" of airstreams in the Northern Hemisphere troposphere and lowermost stratosphere, J. Geophys. Res.-Atmos., 106, 7263–7279, 2001. 8649, 8664

Tong, D. Q., Mathur, R., Kang, D. W., Yu, S. C., Schere, K. L., and Pouliot, G.: Vegetation exposure to ozone over the continental United States: Assessment of exposure indices by the Eta-CMAQ air quality forecast model, Atmos. Environ., 43, 724–733, 2009a. 8648

Tong, D. Q., Muller, N. Z., Kan, H. D., and Mendelsohn, R. O.: Using air quality modeling to study source-receptor relationships between nitrogen oxides emissions and ozone exposures over the United States, Environ. Int., 35, 1109–1117, 2009b. 8650

Tuovinen, J. P., Simpson, D., Emberson, L., Ashmore, M., and Gerosa, G.: Robustness of modelled ozone exposures and doses, Environ. Pollut., 146, 578–586, 2007. 8653, 8658, 8665

USEPA: Air Quality Criteria for Ozone and Other Photochemical Oxidants, Vol. II. EPA-600/P-93/00bF, Epa-600/p-93/00bf, US Environmental Protection Agency, National Center for Environmental Assessment, US Environmental Protection Agency, National Center for Environmental Assessment, Research Triangle Park, NC, 1996. 8647

USEPA: National Ambient Air Quality Standards for Ozone: Proposed Rules, Federal Register, Vol. 75, No. 11, http://www.epa.gov/air/ozonepollution/fr/20100119.pdf, access: 25 July

2010a. 8648

USEPA: Ozone Air Quality Standards, http://www.epa.gov/air/ozonepollution/standards.html, access: 25 July 2010b. 8648

van der Werf, G. R., Randerson, J. T., Giglio, L., Collatz, G. J., Kasibhatla, P. S., and Arellano Jr., A. F.: Interannual variability in global biomass burning emissions from 1997 to 2004, Atmos. Chem. Phys., 6, 3423–3441, doi:10.5194/acp-6-3423-2006, 2006. 8652

Van Dingenen, R., Dentener, F. J., Raes, F., Krol, M. C., Emberson, L., and Cofala, J.: The global impact of ozone on agricultural crop yields under current and future air quality legislation, Atmos. Environ., 43, 604–618, 2009. 8647, 8649, 8650, 8653, 8654, 8658, 8661

Wang, X. P. and Mauzerall, D. L.: Characterizing distributions of surface ozone and its impact on grain production in China, Japan and South Korea: 1990 and 2020, Atmos. Environ., 38, 4383–4402, 2004. 8647, 8653, 8654, 8678

WHO: Air Quality Guidelines for Europe, Reg. Publ. Eur. Ser., WHO Reg. Off. Eur., copenhagen, 2nd edn., 91, 288 pp., 2000. 8648

Wild, O., Pochanart, P., and Akimoto, H.: Trans-Eurasian transport of ozone and its precursors, J. Geophys. Res.-Atmos., 109, D11302, doi:10.1029/2003JD004501, 2004. 8649

Zhang, Q., Streets, D. G., Carmichael, G. R., He, K. B., Huo, H., Kannari, A., Klimont, Z., Park, I. S., Reddy, S., Fu, J. S., Chen, D., Duan, L., Lei, Y., Wang, L. T., and Yao, Z. L.: Asian emissions in 2006 for the NASA INTEX-B mission, Atmos. Chem. Phys., 9, 5131–5153, doi:10.5194/acp-9-5131-2009, 2009. 8649

Zhao, C., Wang, Y. H., Yang, Q., Fu, R., Cunnold, D., and Choi, Y.: Impact of East Asian summer monsoon on the air quality over China: View from space, J. Geophys. Res.-Atmos., 115, D09301, doi:10.1029/2009JD012745, 2010. 8657

Table 1. NO_x emissions totals for each of the receptor regions under the control scenario. Emissions are in $\mathrm{Tg\,yr^{-1}}$.

	Global	N America	SE Asia	Europe
Total	141.2	25.30	29.70	20.40
Anthropogenic	105.2	24.53	27.50	20.02
Biomass Burning	17.77	0.401	1.060	0.206
Natural	18.28	0.364	1.138	0.179

Table 2. AOT40-based yield response functions for 6 widely grown agricultural crops.

Crop	Yield based on weight of	Function (y = relative yield, x = AOT40 in ppm h)	References
Wheat	Grain	$y = -0.0161x + 0.99$	Mills et al. (2007)
Rice	Grain	$y = -0.0039x + 0.94$	Mills et al. (2007)
Maize	Grain	$y = -0.0036x + 1.02$	Mills et al. (2007)
Soybean	Seed	$y = -0.0116x + 1.02$	Mills et al. (2007)
Cotton	Cotton	$y = -0.016x + 1.07$	Mills et al. (2007)
Potato	Tubers	$y = -0.0057x + 0.99$	Mills et al. (2007)

Table 3. M7/M12-based yield response relationships for 4 widely grown agricultural crops.

Crop	Index	Exposure/dose response function: RYL	References
Wheat	M7	$1-\exp[-(\mathrm{M7}/137)^{2.34}]/\exp[-(25/137)^{2.34}]$	Wang and Mauzerall (2004)
Rice	M7	$1-\exp[-(\mathrm{M7}/202)^{2.47}]/\exp[-(25/202)^{2.47}]$	Wang and Mauzerall (2004)
Soybean	M12	$1-\exp[-(\mathrm{M12}/107)^{1.58}]/\exp[-(20/107)^{1.58}]$	Wang and Mauzerall (2004)
Maize	M12	$1-\exp[-(\mathrm{M12}/124)^{2.83}]/\exp[-(20/124)^{2.83}]$	Wang and Mauzerall (2004)

Title Page
Abstract Introduction
Conclusions References
Tables Figures
◀◀ ▶▶
◀ ▶
Back Close
Full Screen / Esc
Printer-friendly Version
Interactive Discussion

Table 4. Summary of regions used and data sources for model intercomparison.

Region	lon, lat (min)	lon, lat (max)	# of stations	References
South-West USA	−125, 30	−110, 40	7	CASTNET Clean air Status and Trends Network (http://java.epa.gov/castnet/epa_jsp/prepackageddata.jsp#ozone)
South-East USA	−90, 25	−80, 35	6	CASTNET Clean air Status and Trends Network (http://java.epa.gov/castnet/epa_jsp/prepackageddata.jsp#ozone)
Great-Lakes USA	−95, 40	−75, 50	16	CASTNET Clean air Status and Trends Network (http://java.epa.gov/castnet/epa_jsp/prepackageddata.jsp#ozone)
Mediterranean	5, 35	30, 45	11	EMEP (http://tarantula.nilu.no/projects/ccc/emepdata.html)
Central Europe	7, 48	17, 54	38	EMEP (http://tarantula.nilu.no/projects/ccc/emepdata.html)
South-East Asia	110, 20	125, 35	3	World Data Centre for Greenhouse Gases (http://gaw.kishou.go.jp/cgi-bin/wdcgg/catalogue.cgi)

Table 5. Regionally-aggregated relative yield loss for the six crops under the control scenario. M7/M12 exposure response relationships were not available for potato and cotton hence for these crops only yield losses based on AOT40 are presented.

CONTROL	WORLD	N AMERICA	SE ASIA	EUROPE
Wheat				
AOT40	5.4	5.1	10.5	1.8
M7	3.6	3.2	5.4	2.7
Rice				
AOT40	1.0	1.7	1.2	0.3
M7	1.0	1.4	1.1	0.9
Maize				
AOT40	1.5	2.0	2.3	0.5
M12	3.6	4.2	4.7	2.8
Soybean				
AOT40	4.3	7.0	5.5	1.7
M12	11.4	15.3	14.5	11.4
Cotton				
AOT40	6.8	8.1	8.5	4.3
Potato				
AOT40	1.4	1.5	3.0	0.5

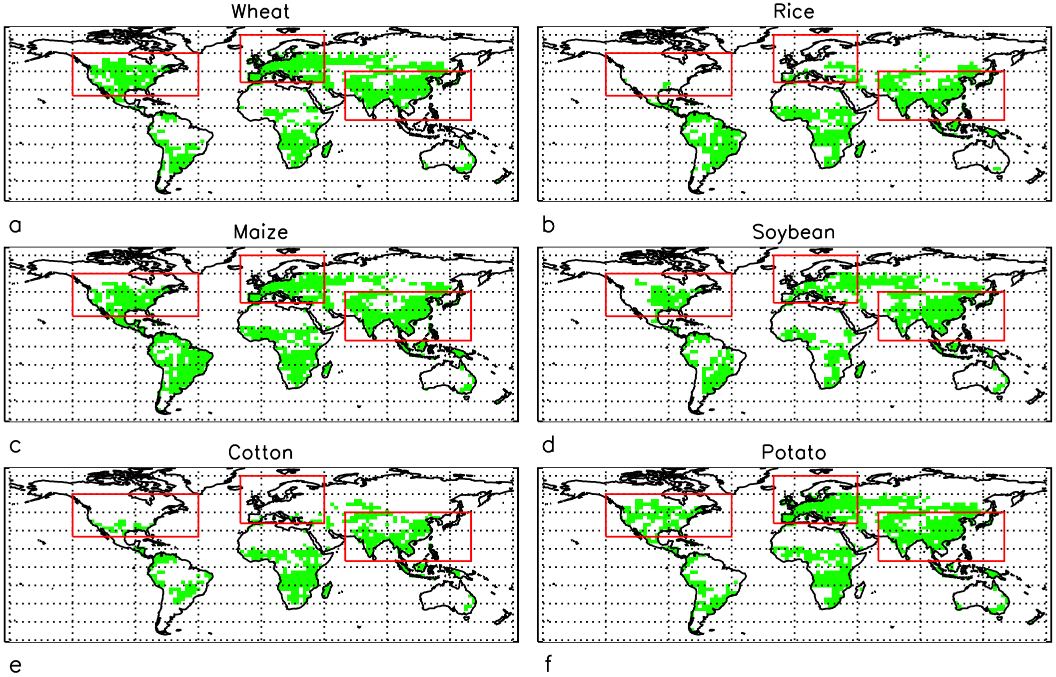

Fig. 1. SAGE group derived crop locations for six major crop types with emissions reduction regions overlaid.

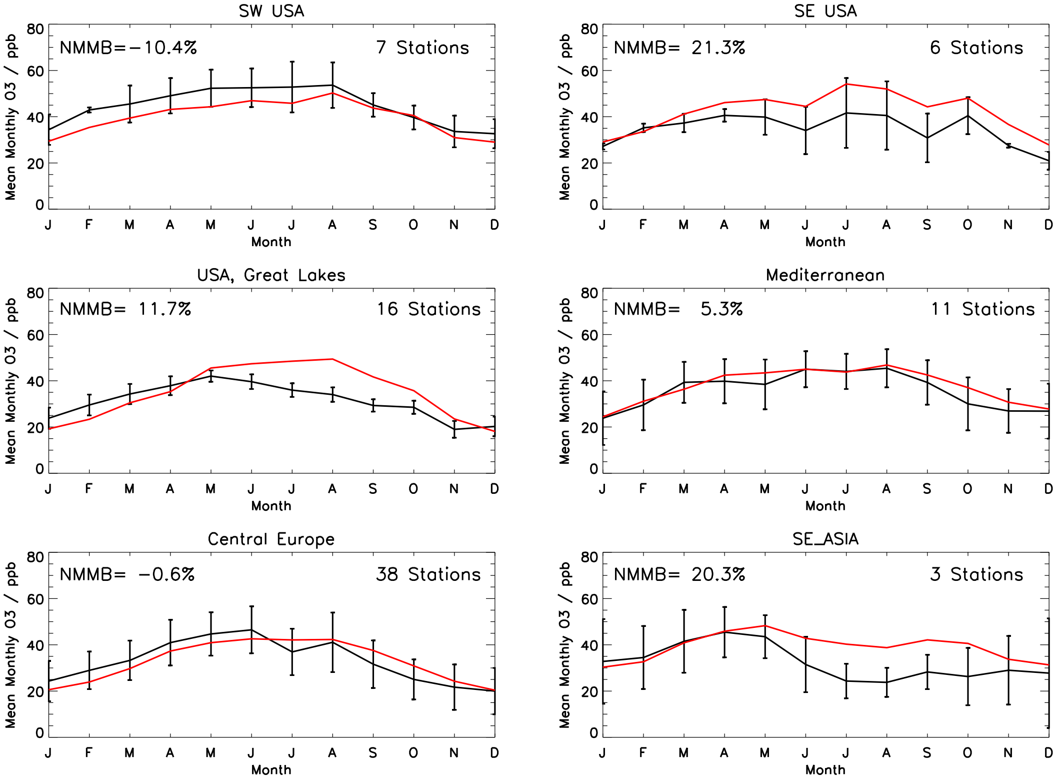

Fig. 2. Comparison between regionally averaged monthly mean surface ozone concentration from monitoring stations (black line) and TOMCAT regional model average under the control scenario (red line) for the year 2000. The model results are the means for the model gridboxes where the stations are located with the model ozone concentration scaled from 30 m (centre of surface gridbox) to 10 m (measurement sample height). Error bars indicate 1 standard deviation on the monthly observational data.

Title Page
Abstract Introduction
Conclusions References
Tables Figures
|◀ ▶|
◀ ▶
Back Close
Full Screen / Esc
Printer-friendly Version
Interactive Discussion

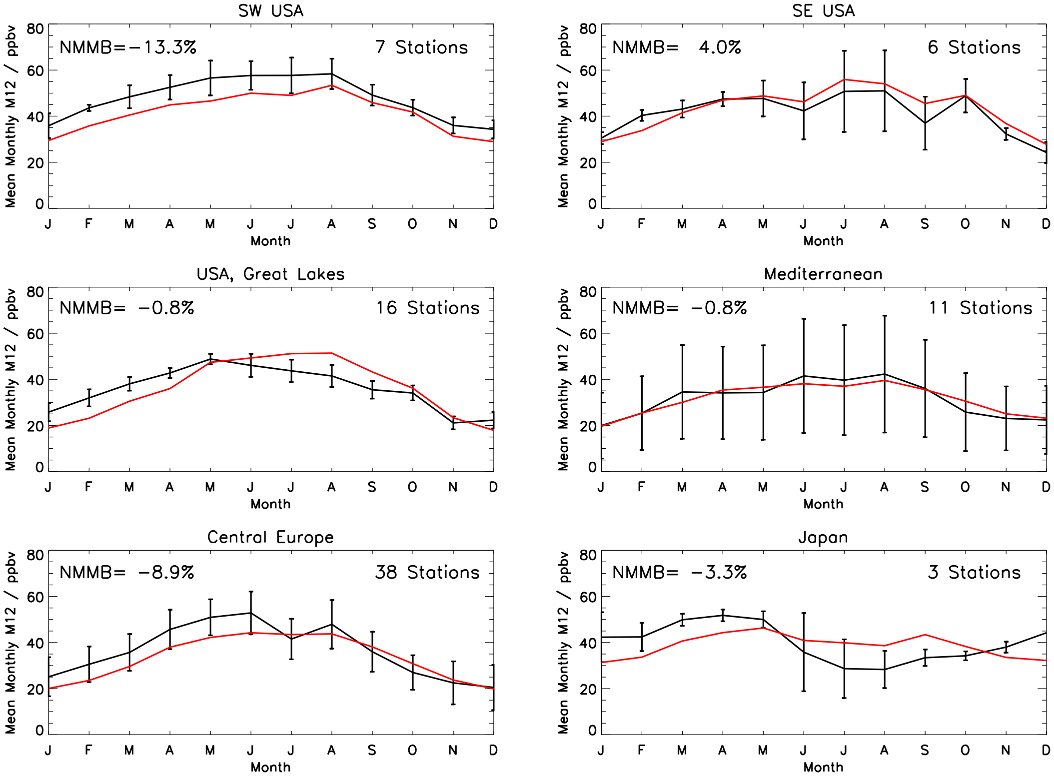

Fig. 3. Comparison between monthly averaged M12 (daytime mean ozone from local time 08:00–19:59) from monitoring stations where hourly ozone data is available (black line) and TOMCAT monthly averaged M12 under the control scenario (red line) for the year 2000. The model results are the means for the model grid boxes where the stations are located with the model ozone concentration scaled from 30m (centre of surface grid box) to 10 m (measurement sample height). Error bars indicate 1 standard deviation on the monthly observational data.

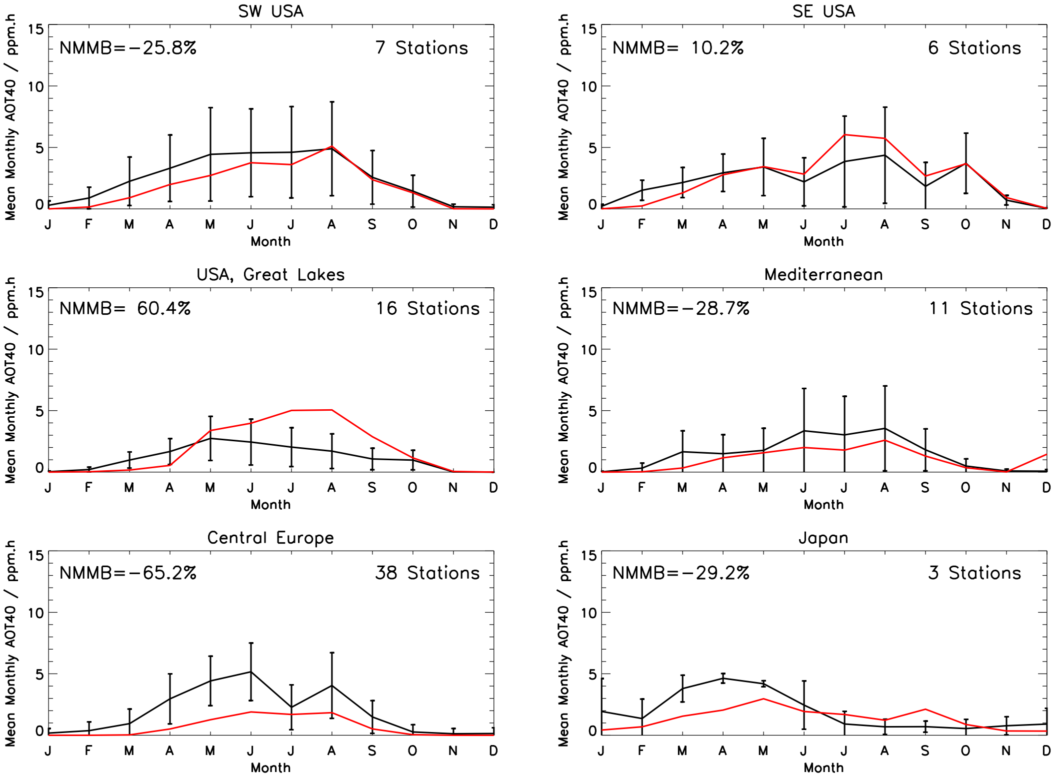

Fig. 4. Comparison between monthly accumulated AOT40 from monitoring stations where hourly ozone data is available (black line) and TOMCAT monthly accumulated AOT40 under the control scenario (red line) for the year 2000. The model results are the means for the model gridboxes where the stations are located with the model ozone concentration scaled from 30 m (centre of surface grid box) to 10 m (measurement sample height). Error bars indicate 1 standard deviation on the monthly observational data.

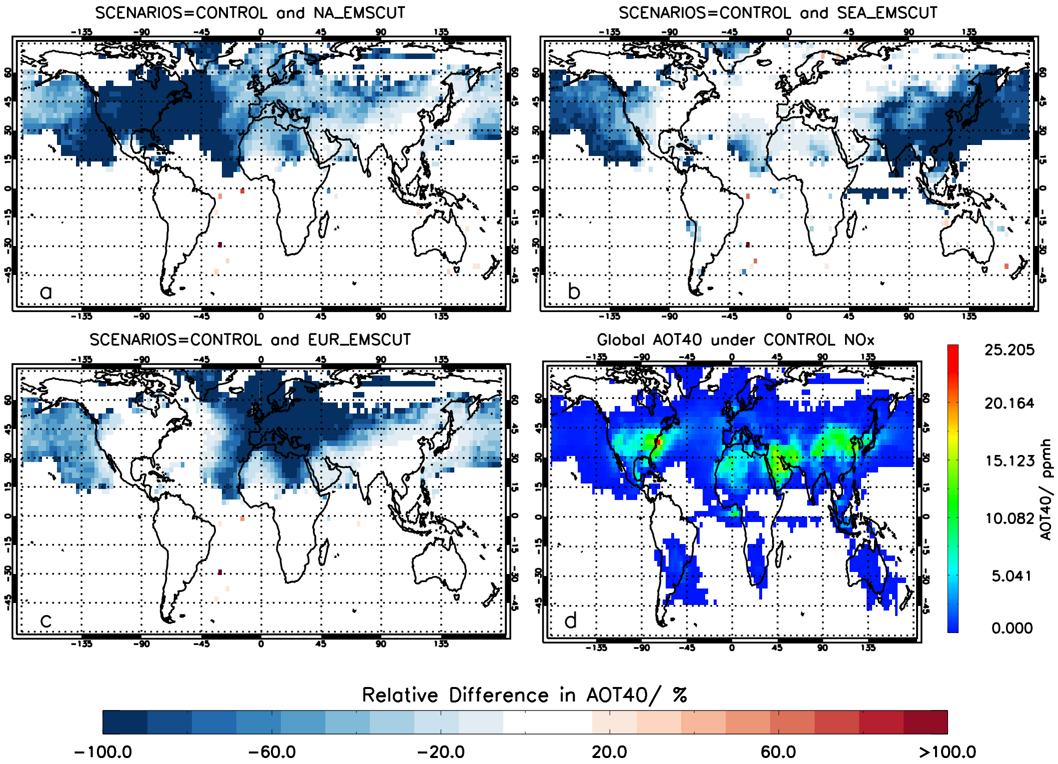

Fig. 5. Relative change in the AOT40 index between the control and each of the emissions reduction scenarios **(a–c)** with AOT40 under the control scenario shown for reference **(d)**.

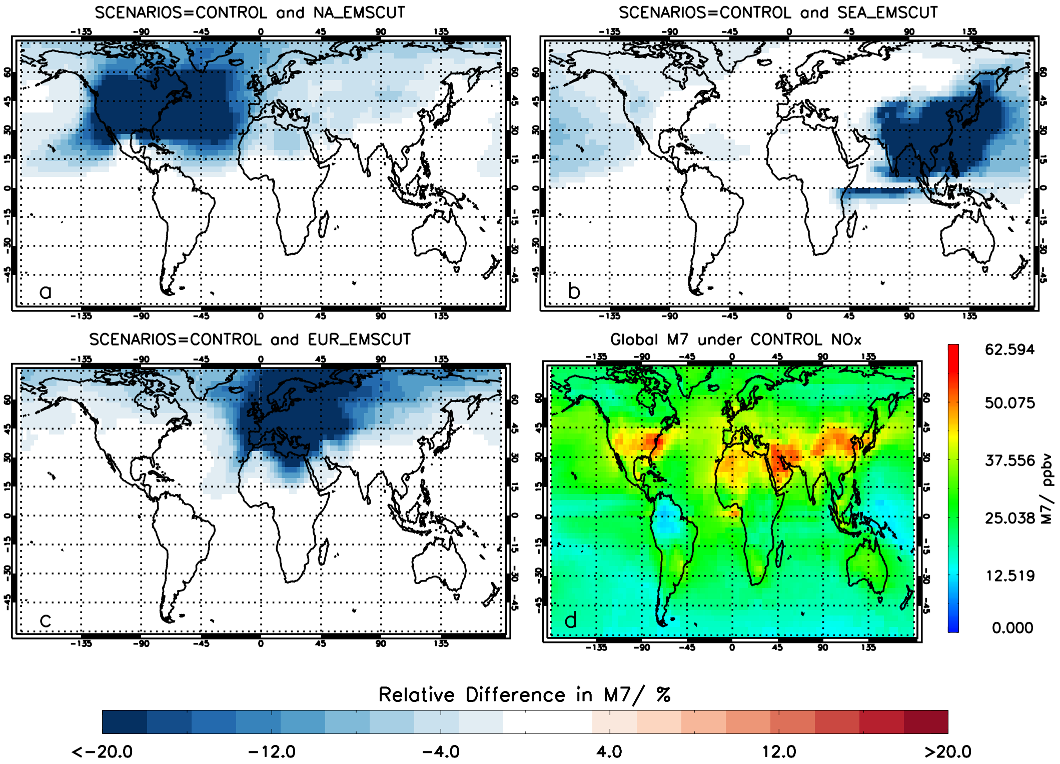

Fig. 6. Relative change in the M7 index between the control and each of the emissions reduction scenarios **(a–c)** with M7 under the control scenario shown for reference **(d)**.

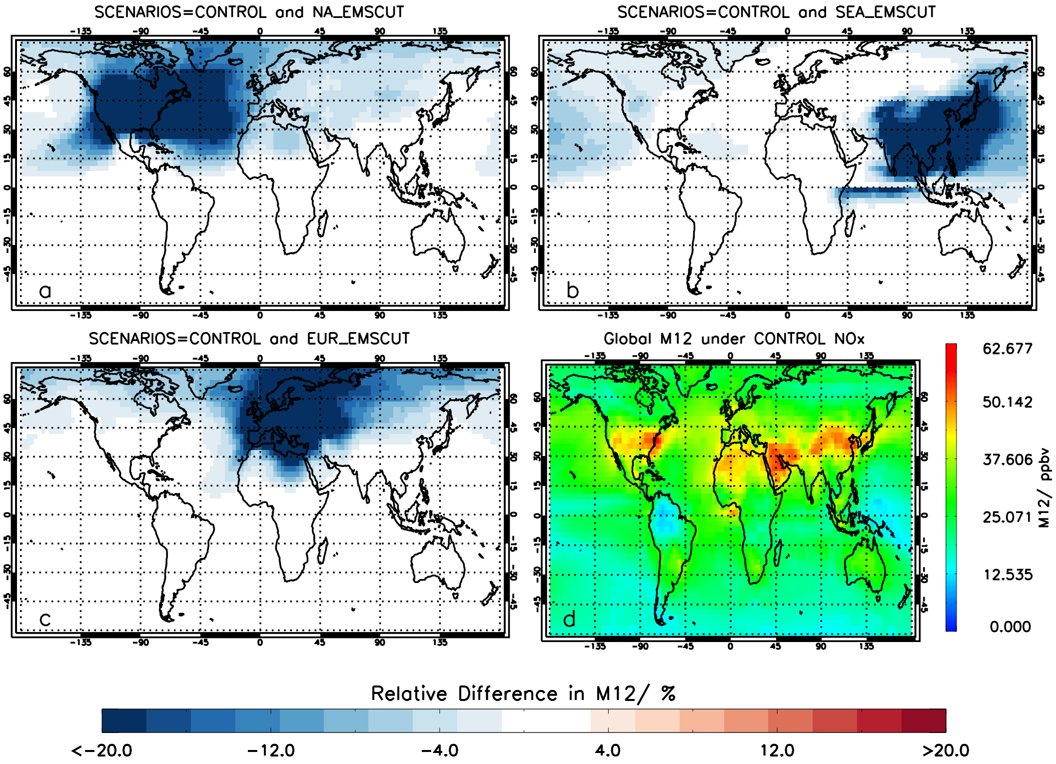

Fig. 7. Relative change in the M12 index between the control and each of the emissions reduction scenarios **(a–c)** with M12 under the control scenario shown for reference **(d)**.

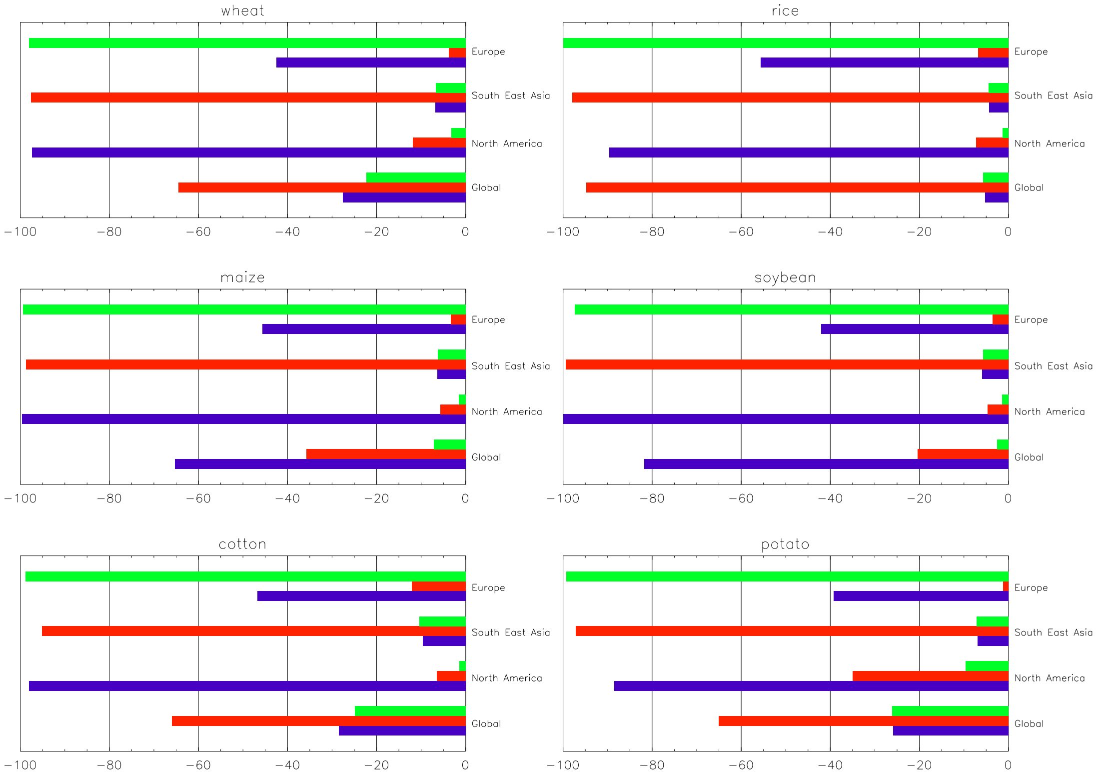

Fig. 8. Percentage reductions in ozone-induced relative yield loss for 6 major crops (based upon the AOT40 exposure index) resulting from regional cuts in NO_x emissions. The y-axis shows the receptor regions with the coloured bars indicating the changes under each emissions scenario compared to the control (Green = Europe, Red = SE Asia and Blue = N America).

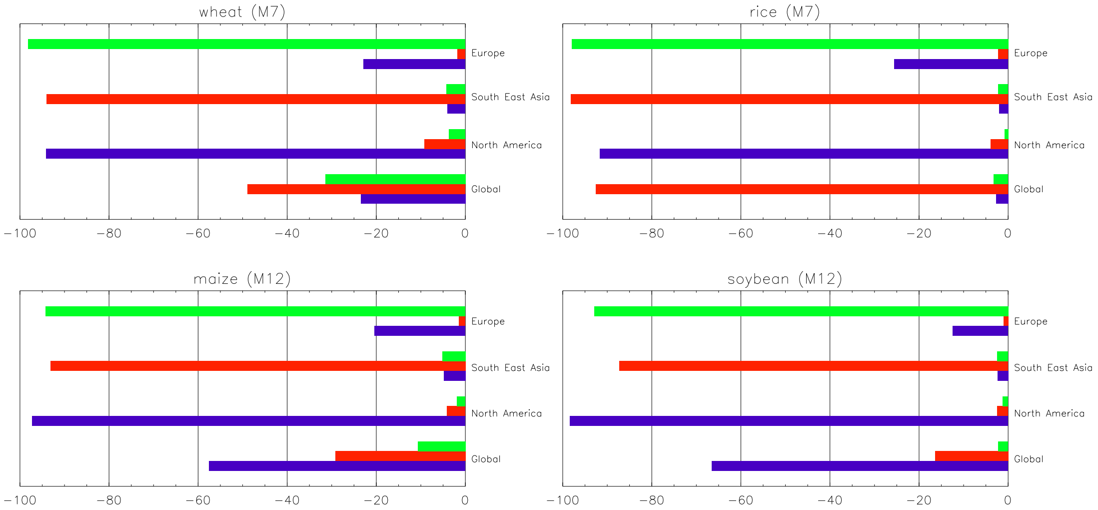

Fig. 9. Percentage reductions in ozone-induced relative yield loss for 4 major crops (based upon the M7/M12 exposure indices) resulting from regional cuts in NO_x emissions. The y-axis shows the receptor regions with the coloured bars indicating the changes under each emissions scenario compared to the control (Green = Europe, Red = SE Asia and Blue = N America).

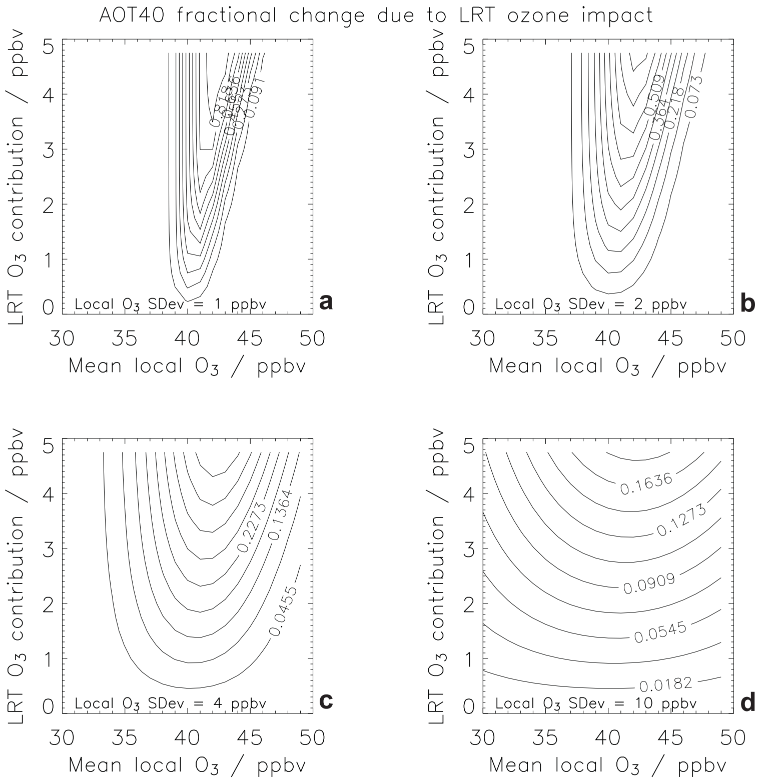

Fig. 10. Fractional change in AOT40 due to long-range transport (LRT) ozone as a function of mean local ozone and LRT ozone contribution. The panels **(a–d)** show different standard deviations of the local ozone distribution. Local ozone is assumed to be normally distributed, and the LRT contribution is assumed to uniformly translate the local ozone distribution across all concentrations. AOT40 is assumed proportional to the fraction of distribution concentrations exceeding 40 ppbv.

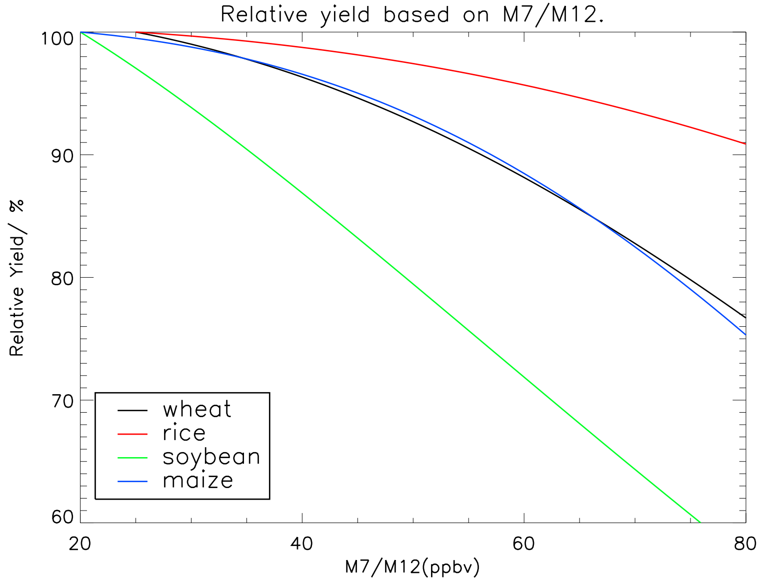

Fig. 11. Relative yield as a function of M7/M12 for wheat, rice, maize and soybean. The equations for these functions are shown in Table 3.